



Cite this: *Polym. Chem.*, 2016, 7, 7316

## Dihydroxyanthraquinone derivatives: natural dyes as blue-light-sensitive versatile photoinitiators of photopolymerization†

Jing Zhang,<sup>a</sup> Jacques Lalevée,<sup>b</sup> Jiacheng Zhao,<sup>a</sup> Bernadette Graff,<sup>b</sup> Martina H. Stenzel\*<sup>a</sup> and Pu Xiao\*<sup>a</sup>

Four dihydroxyanthraquinone derivatives [*i.e.* 1,2-dihydroxyanthraquinone (12-DHAQ), 1,4-dihydroxyanthraquinone (14-DHAQ), 1,5-dihydroxyanthraquinone (15-DHAQ), and 1,8-dihydroxyanthraquinone (18-DHAQ)], when combined with various additives (*e.g.* iodonium salt, tertiary amine, *N*-vinylcarbazole, phenacyl bromide, and 4-cyanopentanoic acid dithiobenzoate), are investigated as photoinitiating systems for free radical photopolymerization [*e.g.* cross-linked free radical photopolymerization of multifunctional monomers or reversible addition–fragmentation chain transfer (RAFT) photopolymerization of mono-functional monomers] and cationic photopolymerization. 14-DHAQ, 15-DHAQ and 18-DHAQ exhibit good solubility in solvent (acetonitrile) and monomers (methacrylate and epoxide) and demonstrate absorption maxima in the blue light wavelength range, which makes them potential candidates to work under the irradiation of a household blue LED bulb. Among all the investigated dihydroxyanthraquinone derivative-based photoinitiating systems, 18-DHAQ based systems exhibit the highest photoinitiating ability for both free radical and cationic photopolymerization while 12-DHAQ based systems are inefficient. It illustrates that the positions of hydroxyl substituents in the anthraquinone molecule play a significant role in the photoinitiating ability of dihydroxyanthraquinone derivatives. The photochemical mechanisms are investigated by fluorescence, laser flash photolysis, steady state photolysis, and electron spin resonance spin trapping techniques, and the results are in agreement with the relevant photopolymerization efficiency.

Received 5th September 2016

Accepted 16th October 2016

DOI: 10.1039/c6py01550f

www.rsc.org/polymers

### Introduction

The nature of the photoinitiator (PI) is central in a photoinitiating system (PIS) as the PI determines the wavelengths of

light in which the polymerization can be carried out. In multi-component PISs, the PI subsequently interacts with relevant additives through electron transfer or energy transfer reactions to generate active species (*e.g.* radicals or cations) for the initiation of various types of photopolymerization reactions.<sup>1–5</sup> Visible light-induced polymerization is a promising approach in the fabrication of polymeric materials<sup>6–12</sup> under green chemistry conditions since the radicals or cations are generated under mild conditions. The performance of the photoinitiator is crucial since it does not only affect the photopolymerization process but also influences the final properties of the fabricated polymeric material, *e.g.* polyoxometalate-based photoinitiators can affect the final mechanical properties of the fabricated polymeric materials.<sup>13,14</sup> Furthermore, natural dyes may act as highly interesting photoinitiators as they are widely abundant and in addition display often low toxicity, ideal for the synthesis of biomaterials. Very recently, it has been reported that curcumin (a yellow-orange natural dye derived from the rhizomes of *Curcuma longa*) based PISs demonstrated excellent photoinitiating ability for the free radical photopolymerization of methacrylates.<sup>15</sup> More

<sup>a</sup>Centre for Advanced Macromolecular Design, School of Chemistry, University of New South Wales, Sydney, NSW 2052, Australia. E-mail: m.stenzel@unsw.edu.au, p.xiao@unsw.edu.au

<sup>b</sup>Institut de Science des Matériaux de Mulhouse IS2M, UMR CNRS 7361, ENSCMu-UHA, 15, rue Jean Starcky, 68057 Mulhouse Cedex, France

† Electronic supplementary information (ESI) available: UV-vis absorption of 12-DHAQ (Fig. S1); emission spectra of blue and green LED bulbs, and their overlap with the absorption spectra of DHAQs (Fig. S2); IR spectra recorded before and after the photopolymerization of the Bis-GMA/TEGDMA blend upon exposure to the household blue LED bulb (Fig. S3); photopolymerization profile of the Bis-GMA/TEGDMA blend in laminate or under air in the presence of 18-DHAQ/Iod/NVK upon exposure to the blue LED bulb (Fig. S4); steady state photolysis of 15-DHAQ/Iod, 18-DHAQ/Iod and 18-DHAQ/Iod/NVK in acetonitrile under irradiation of the blue LED bulb (Fig. S5); fluorescence quenching of 15-DHAQ by TEOH in acetonitrile (Fig. S6); laser flash photolysis of 18-DHAQ (Fig. S7); IR spectra recorded before and after the photopolymerization of EPOX upon exposure to the household blue LED bulb (Fig. S8). See DOI: 10.1039/c6py01550f

interestingly, the crosslinked polymethacrylates fabricated using the curcumin-based PIS exhibited no toxicity to human fibroblast HS-27 cells, endowing it with great potential for the production of biocompatible polymeric materials.<sup>15</sup> This promising result inspired us to investigate further the possibility of other natural dyes to initiate various types of photopolymerizations.

9,10-Anthraquinone derivatives (AQs) are a family of natural dyes derived from plants and other biological sources.<sup>16</sup> They have attracted significant attention due to their widespread applications ranging from textile dyeing and paints to food coloring and medical treatments (*e.g.* anticancer properties, post-partum tonic and aphrodisiac), to name but a few.<sup>17,18</sup> Specifically, 1,8-dihydroxyanthraquinone (18-DHAQ) is a component of the chromophore of hypericin from the plants of the *Hypericum* genus and it finds applications in the photodynamical therapy of cancer.<sup>19</sup> Moreover, 12-DHAQ, 14-DHAQ and 18-DHAQ can also bind to DNA and therefore act as anticancer drugs.<sup>18</sup> Even though 1,4-bis(pentylamino)anthraquinone (oil blue N, OBN) based PISs were found to be efficient PISs for cationic photopolymerization under red laser diode (635 nm) irradiation, the photoinitiation efficiency for free radical photopolymerization was very low.<sup>20</sup> Furthermore, to the best of our knowledge, dihydroxyanthraquinone derivative-based PISs have not yet been described as efficient initiators. Therefore, it is interesting and valuable to investigate different dihydroxyanthraquinone derivative-based PISs and the effect of chemical structures on their photoinitiation efficiency. The investigation will clarify the relationship of the chemical structures/photoinitiation efficiency of dihydroxyanthraquinone derivatives as photoinitiators of polymerization, which can expand the knowledge of both polymer and photochemistry fields.

In this study the photoinitiating ability of four dihydroxyanthraquinone derivatives (1,2-dihydroxyanthraquinone, 1,4-dihydroxyanthraquinone, 1,5-dihydroxyanthraquinone, and 1,8-dihydroxyanthraquinone), along with various additives, to initiate both free radical (uncontrolled free radical photopolymerization or RAFT photopolymerization) and cationic photopolymerization upon exposure to a blue LED bulb has been investigated. Furthermore, the mechanism of the photochemical reaction between the dihydroxyanthraquinone derivatives and additives is investigated and discussed in detail.

## Experimental section

### Materials

The investigated dihydroxyanthraquinone derivatives (DHAQs) were obtained from different companies, *i.e.* 1,2-dihydroxyanthraquinone (12-DHAQ; BAYER), 1,4-dihydroxyanthraquinone (14-DHAQ; L. LIGHT & Co. Ltd), 1,5-dihydroxyanthraquinone (15-DHAQ; Aldrich), and 1,8-dihydroxyanthraquinone (18-DHAQ; Aldrich), and are shown in Scheme 1. Diphenyliodonium hexafluorophosphate (Iod), *N*-vinylcarbazole (NVK), triethanol-



**Scheme 1** Chemical structures of the investigated dihydroxyanthraquinone derivatives (12-DHAQ, 14-DHAQ, 15-DHAQ and 18-DHAQ).

amine (TEAOH) and phenacyl bromide (R-Br) were purchased from Sigma-Aldrich and used as additives (Scheme 2) for the photoinitiating systems. (3,4-Epoxy)cyclohexane)methyl 3,4-epoxycyclohexylcarboxylate (EPOX), bisphenol A glycerolate dimethacrylate (Bis-GMA) and triethylene glycol dimethacrylate (TEGDMA) were also obtained from Sigma-Aldrich and used as benchmark monomers (Scheme 2) for cationic photopolymerization and free radical photopolymerization. Di(ethylene glycol) methyl ether methacrylate (DEGMEMA) was purchased from Sigma-Aldrich and passed over basic aluminum oxide to remove the inhibitor. 4-Cyanopentanoic acid dithiobenzoate (CPADB) was synthesized according to a reported procedure<sup>21</sup> and used as a RAFT agent.

### Computational procedure

Molecular orbital calculations were carried out with the Gaussian 03 package. The electronic absorption spectra of the different compounds were calculated with the time-dependent density functional theory at the B3LYP/6-31G\* level on the relaxed geometries calculated at the UB3LYP/6-31G\* level; the molecular orbitals involved in these transitions can be extracted.<sup>22,23</sup> The geometries were frequency checked.

### Irradiation sources

Two household LED bulbs were used as irradiation devices: a blue LED bulb (emission wavelength centered at 455 nm; incident light intensity: 100 mW cm<sup>-2</sup>) and a green LED bulb (518 nm; 60 mW cm<sup>-2</sup>).

### Photopolymerization of multifunctional monomers

The photopolymerization reactions of the multifunctional monomers in the presence of different DHAQ-based photoinitiating systems upon exposure to the household LED bulbs were monitored using an ATR-IR (BRUKER, IFS 66/s). Specifically, a layer of liquid formulation (~20 μm thick) was coated on the surface of the ATR horizontal crystal and the ATR-IR spectra of the sample were recorded at different time intervals during the household LED irradiation. The evolution of the epoxy group content of EPOX and the double bond content of the Bis-GMA/TEGDMA (70%/30%, wt%) blend were followed by ATR-IR spectroscopy using the bands at about 790 cm<sup>-1</sup> and 1635 cm<sup>-1</sup>, respectively.<sup>24</sup> The cationic photopolymerization of EPOX was carried out exposed to the air, while the free radical photopolymerization of methacrylates was conducted in laminate. The degree of the epoxy group or double bond conversion *C* at time *t* during the photopolymerization is calculated from  $C = (A_0 - A_t)/A_0 \times 100\%$



**Scheme 2** Chemical structures of the investigated additives (Iod, NVK, TEOAH, R-Br, and CPADB) of photoinitiating systems and the studied monomers (Bis-GMA, TEGDMA, DEGMEMA and EPOX).

(where  $A_0$  is the initial peak area before irradiation and  $A_t$  is the peak area of the functional groups at time  $t$ ). The conversion  $C$  measured here is not throughout the whole sample thickness as the penetration depth of an infrared beam in the sample is *ca.* 0.5–3  $\mu\text{m}$  for the ATR-IR spectroscopy. In addition, the conversions measured here can be used to evaluate the photoinitiation efficiency of the relevant DHAQ-based photoinitiating systems. Well-known blue-light-sensitive camphorquinone-based photoinitiating systems were used as references.

### Fluorescence experiments

The fluorescence properties of DHAQs in acetonitrile were studied using a Cary Eclipse Fluorescence Spectrophotometer (Agilent Technologies). The fluorescence quenching of DHAQs by additives (*i.e.* Iod or TEOAH) was investigated from the classical Stern–Volmer treatment<sup>25</sup> ( $I_0/I = 1 + k_q\tau_0[\text{additive}]$ ; where  $I_0$  and  $I$  stand for the fluorescence intensity of DHAQs in the absence and the presence of the additives, respectively;  $\tau_0$  stands for the lifetime of DHAQs in the absence of additives).

### Laser flash photolysis

Nanosecond laser flash photolysis (LFP) experiments were carried out using a Q-switched nanosecond Nd/YAG laser ( $\lambda_{\text{exc}} = 355 \text{ nm}$ , 9 ns pulses; energy reduced down to 10 mJ) from Continuum (Minilite) and an analyzing system consisting of a ceramic xenon lamp, a monochromator, a fast photomultiplier and a transient digitizer (Luzchem LFP 212).<sup>26</sup>

### Steady state photolysis experiments

DHAQs in the presence of additives (*i.e.* Iod or TEOAH) in acetonitrile were irradiated with a blue LED bulb, and the UV-vis spectra were recorded using a Cary 300 UV-VIS Spectrophotometer at different irradiation time.

### ESR spin trapping (ESR-ST) experiments

ESR-ST experiments were carried out using a Bruker EMX-plus X-Band ESR Spectrometer. The radicals were generated

at room temperature upon blue LED exposure under argon and trapped by phenyl-*N-tert*-butylnitron (PBN) according to a procedure<sup>27</sup> described elsewhere in detail. The ESR spectral simulations were carried out with the WINSIM software.

### Photopolymerization of a monofunctional monomer

DHAQ-based photoinitiating systems were dissolved in a monofunctional monomer DEGMEMA in a 25 mL clear round glass bottle with a rubber cover and then the formulations were bubbled with argon for 30 minutes to remove oxygen. After being irradiated with a blue LED bulb ( $50 \text{ mW cm}^{-2}$ ) for several hours, the formulations were poured into a large excess of diethyl ether to precipitate the synthesized poly (DEGMEMA). Finally, poly(DEGMEMA) was dried under vacuum for 24 h.

### Size exclusion chromatography (SEC)

The molecular weight and polydispersity of the synthesized poly(DEGMEMA) were analyzed *via* size exclusion chromatography (SEC). SEC was implemented using a Shimadzu modular system comprising a DGU-12A degasser, an LC-10AT pump, an SIL-10AD automatic injector, a CTO-10A column oven, an RID-10A refractive index detector, and an SPD-10A Shimadzu UV/vis detector. A Phenomenex  $50 \times 7.8 \text{ mm}$  guard column and four Phenogel  $300 \times 7.8 \text{ mm}$  linear columns ( $500, 10^3, 10^4, \text{ and } 10^5 \text{ \AA}$  pore size,  $5 \mu\text{m}$  particle size) were used for the analyses. Tetrahydrofuran (THF; HPLC grade) at a flow rate of  $1 \text{ mL min}^{-1}$  and a constant temperature of  $50 \text{ }^\circ\text{C}$  was used as the mobile phase with an injection volume of  $50 \mu\text{L}$ . The samples were filtered through  $0.45 \mu\text{m}$  filters. The unit was calibrated using commercially available linear polystyrene standards ( $0.5\text{--}1000 \text{ kDa}$ , Polymer Laboratories). Chromatograms were processed using the Cirrus 2.0 software (Polymer Laboratories).

## Results and discussion

### Light absorption properties of DHAQs

The light absorption properties of DHAQs (*i.e.* 12-DHAQ, 14-DHAQ, 15-DHAQ and 18-DHAQ) in acetonitrile are shown in Fig. 1 and S1 in the ESI,<sup>†</sup> while their absorption maxima ( $\lambda_{\max}$ ) and extinction coefficients ( $\epsilon$ ) at  $\lambda_{\max}$  and at the maximum emission wavelengths of household blue and green LEDs are summarized in Table 1. As illustrated in Fig. 1, 14-DHAQ, 15-DHAQ and 18-DHAQ exhibit absorption maxima ( $\lambda_{\max}$ ) at 477 nm, 417 nm and 426 nm with the corresponding extinction coefficient of approximately  $7000 \text{ M}^{-1} \text{ cm}^{-1}$ . However, it is difficult to determine exactly the extinction coefficient of 12-DHAQ due to its low solubility in acetonitrile (Fig. S1 in the ESI<sup>†</sup>). Interestingly, the light absorption of 14-DHAQ, 15-DHAQ and 18-DHAQ demonstrates an intense overlap with the emission spectrum of a household blue LED bulb (Fig. S2 in the ESI;<sup>†</sup> Table 1), which makes them potential photoinitiators under the blue LED bulb. In addition, the light absorption of 14-DHAQ overlaps sufficiently with the emission spectrum of the green LED bulb: this feature endows this dye with the potential to be used under longer-wavelength LEDs.

The molecular orbitals of the different DHAQs involved in their lowest energy absorption band (HOMO  $\rightarrow$  LUMO) are illustrated in Fig. 2. A charge transfer character was found for the lowest energy transition *i.e.* from the hydroxyl group (for the Highest Occupied Molecular Orbital – HOMO) to the



Fig. 1 UV-vis absorption spectra of 14-DHAQ, 15-DHAQ and 18-DHAQ in acetonitrile.

Table 1 Light absorption properties of the studied anthraquinone derivatives: absorption maxima  $\lambda_{\max}$ , extinction coefficients at  $\lambda_{\max}$  and at the maximum emission wavelengths of the different LED bulbs

|         | $\lambda_{\max}$<br>(nm) | $\epsilon_{\max}$<br>( $\text{M}^{-1} \text{ cm}^{-1}$ ) | $\epsilon_{455 \text{ nm}}^a$<br>( $\text{M}^{-1} \text{ cm}^{-1}$ ) | $\epsilon_{518 \text{ nm}}^a$<br>( $\text{M}^{-1} \text{ cm}^{-1}$ ) |
|---------|--------------------------|--|--|--|
| 14-DHAQ | 477                      | 7200   | 7000   | 3000   |
| 15-DHAQ | 417                      | 7000   | 3500   | 150  |
| 18-DHAQ | 426                      | 6700   | 3900   | 50   |

<sup>a</sup> For different LEDs.

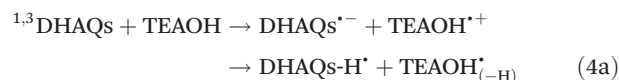


Fig. 2 Highest occupied molecular orbital (HOMO) and the lowest unoccupied molecular orbital (LUMO) of 12-DHAQ, 14-DHAQ, 15-DHAQ and 18-DHAQ at the UB3LYP/6-31G\* level (isovalue = 0.02).

anthraquinone moiety (for the Lowest Unoccupied Molecular Orbital – LUMO) for all compounds. Interestingly, the participation of two hydroxyl groups as electron donors to the HOMO can be easily found for 14-DHAQ, which is in full agreement with the red-shifted light absorption properties of this compound compared to other DHAQs.

### Free radical photopolymerization of multifunctional monomers and relevant photochemical mechanisms on DHAQ-based photoinitiating systems

As demonstrated above, 14-DHAQ, 15-DHAQ and 18-DHAQ can absorb blue light from the LED and the corresponding generated excited states of DHAQs are expected to interact with additives (*e.g.* Iod or TEOOH) to produce radicals in reactions (1)–(4) as reported previously.<sup>3</sup>



For instance, radicals generated from 14-DHAQ/Iod (phenyl radicals  $\text{Ph}^{\bullet}$ , reaction (3)) or 14-DHAQ/TEAOH (aminoalkyl radicals  $\text{TEAOH}^{\bullet(-\text{H})}$ , reaction (4a)) two-component photoinitiating systems upon blue LED exposure can initiate free radical photopolymerization of methacrylates (*i.e.* Bis-GMA/TEGDMA blend) in laminate as illustrated in Fig. 3. 36% and 28% of methacrylate conversion were achieved after 300 s of blue LED irradiation in the presence of 14-DHAQ/Iod and 14-DHAQ/TEAOH systems respectively. Interestingly, the polymerization rate and conversion were significantly promoted by the addition of a third component into the photoinitiating systems as demonstrated in Fig. 3 and Table 2. In this case, new types of radicals were produced as in reactions (5)–(7) to



Fig. 3 Photopolymerization profiles (conversions of methacrylate functions (C) vs. time; measured with ATR-IR) of the Bis-GMA/TEGDMA blend (70%/30%, w/w) in laminate in the presence of (a) DHAQ/Iod/NVK (0.5%/2%/3%, wt%) and (b) DHAQ/TEAOH/R-Br (0.5%/2%/3%, wt%) upon exposure to the blue LED@455 nm; CQ/Iod (0.5%/2%, wt%) and CQ/TEAOH (0.5%/2%, wt%) as references.

Table 2 Bis-GMA/TEGDMA blend (70%/30%, wt%) or EPOX conversions (measured with ATR-IR) obtained upon exposure to the household blue LED bulb at 455 nm in the presence of dihydroxyanthraquinone derivative-based PISs (DHAQs: 0.5 wt%; Iod or TEOH: 2 wt%; NVK or R-Br: 3 wt%; CQ/Iod (0.5%/2%, wt%) and CQ/TEAOH (0.5%/2%, wt%) as references)

| PISs               | Conversion (C) of monomers at different LED irradiation time |           |           |           |
|--------------------|--|-----------|-----------|-----------|
|                    | Bis-GMA/TEGDMA   |           | EPOX      |           |
|                    | C (10 s)   | C (300 s) | C (120 s) | C (800 s) |
| Iod                | 0  | 0         | 0         | 0         |
| NVK                | 0  | 0         | 0         | 0         |
| 14-DHAQ/Iod        | 14%  | 36%       | 0         | 0         |
| 14-DHAQ/Iod/NVK    | 22%  | 50%       | 15%       | 67%       |
| 18-DHAQ/Iod/NVK    | 24%  | 55%       | 62%       | 79%       |
| 15-DHAQ/Iod/NVK    | 3%   | 42%       | 0         | 15%       |
| 12-DHAQ/Iod/NVK    | 0  | 0         | 0         | 0         |
| CQ/Iod             | 15%  | 57%       | 0         | 0         |
| TEAOH              | 0  | 0         |           |           |
| R-Br               | 0  | 0         |           |           |
| 14-DHAQ/TEAOH      | 0  | 28%       |           |           |
| 14-DHAQ/TEAOH/R-Br | 4%   | 48%       |           |           |
| 18-DHAQ/TEAOH/R-Br | 4%   | 56%       |           |           |
| 15-DHAQ/TEAOH/R-Br | ~0   | 38%       |           |           |
| 12-DHAQ/TEAOH/R-Br | 0  | 0         |           |           |
| CQ/TEAOH           | 14%  | 45%       |           |           |

initiate the free radical polymerization of the methacrylate.<sup>28</sup> More specifically, 50% and 48% of methacrylate conversion was attained in the presence of 14-DHAQ/Iod/NVK and 14-DHAQ/TEAOH/R-Br, respectively. 15-DHAQ and 18-DHAQ based three-component photoinitiating systems were also capable of initiating the polymerization of methacrylates, with 15-DHAQ being less efficient and 18-DHAQ more efficient than the 14-DHAQ based three-component system. Markedly, 18-DHAQ/Iod/NVK and 18-DHAQ/TEAOH/R-Br systems even led to higher methacrylate conversion than the well-known camphorquinone CQ/tertiary amine (TEAOH) system under the blue LED irradiation (Fig. 3 and Table 2). Furthermore, from the IR spectra (Fig. S3 in the ESI†), the dramatic decrease of the vinyl group ( $\sim 1635\text{ cm}^{-1}$ ) indicated clearly the efficient

photopolymerization reaction. In addition to the photopolymerization in laminate, the 18-DHAQ/Iod/NVK system also initiated the polymerization of methacrylate under air (Fig. S4 in the ESI†) but the system led to lower conversion (24%) after 300 s of blue LED irradiation due to the continuous diffusion of oxygen into the sample (*i.e.* the oxygen inhibition effect for free radical polymerization).



More interestingly, 14-DHAQ/Iod/NVK and 18-DHAQ/Iod/NVK systems can also work under green LED (518 nm) irradiation for the polymerization of methacrylates (Fig. 4). Higher polymerization rates and conversions can be achieved in the presence of the 14-DHAQ based system than that of the 18-DHAQ based system, which can be attributed to the fact that the light absorption of 14-DHAQ exhibits more overlapping



Fig. 4 Photopolymerization profiles (C vs. time; measured with ATR-IR) of the Bis-GMA/TEGDMA blend (70%/30%, w/w) in laminate in the presence of DHAQ/Iod/NVK (0.5%/2%/3%, wt%) upon exposure to the green LED@518 nm.

with the emission spectrum of the green LED bulb than that of 18-DHAQ (Fig. S2 in the ESI†).

As expected, 12-DHAQ based photoinitiating systems were ineffective for free radical polymerization due to their low solubility in the Bis-GMA/TEGDMA blend. In addition, the additives (*i.e.* Iod, NVK, TEOH and R-Br) without the presence of DHAQs cannot initiate the photopolymerization under blue LED irradiation indicating the important role of DHAQs in the systems. We therefore further investigated the relevant photochemical mechanisms for the radical generation of DHAQ-based photoinitiating systems.

As the photophysical and photochemical properties of DHAQs have been widely investigated,<sup>19,29–31</sup> the focus of this work was to investigate the underpinning mechanisms for the production of radicals in the DHAQ-based photoinitiating systems. Addition of TEOH to the solutions of 15-DHAQ or 18-DHAQ in acetonitrile led to significant decrease in the fluorescence intensity of the DHAQs (*e.g.* the fluorescence quenching experiments on 15-DHAQ, Fig. S6 in the ESI,†  $k_q\tau_0 = 7.25 \text{ M}^{-1}$ ; for 18-DHAQ/TEOH,  $k_q\tau_0 = 7.23 \text{ M}^{-1}$ ), which indicated the electron transfer interaction between the excited singlet state of DHAQs and the ground-state TEOH as in reaction (4a).<sup>29</sup> The <sup>1</sup>DHAQ/TEOH interaction is almost diffusion-controlled as indicated by the interaction rate constant (*e.g.*  $k_q > 9 \times 10^8 \text{ M}^{-1} \text{ s}^{-1}$  for <sup>1</sup>18-DHAQ/TEOH). However, there is no correlation between the UV-vis absorption properties of 15-DHAQ *vs.* 18-DHAQ (*i.e.*  $\epsilon_{455 \text{ nm}} = 3500 \text{ M}^{-1} \text{ cm}^{-1}$  and  $3900 \text{ M}^{-1} \text{ cm}^{-1}$  for 15-DHAQ and 18-DHAQ, respectively; Table 1) and their relevant photopolymerization efficiency, *i.e.* 15-DHAQ and 18-DHAQ based photoinitiating systems exhibited the lowest and the highest photoinitiation ability, respectively, but they have similar light absorption properties. Furthermore, the electron transfer quantum yields [ $\Phi_{\text{eT}} = k_q\tau_0 [\text{TEOH}]/(1 + k_q\tau_0 [\text{TEOH}])$ ],<sup>1</sup> where  $[\text{TEOH}] = 1.34 \times 10^{-1} \text{ M}$ ] of 15-DHAQ/TEOH ( $\Phi_{\text{eT}} = 0.493$ ) and 18-DHAQ/TEOH ( $\Phi_{\text{eT}} = 0.492$ ) are also quite similar which would result in similar yields of aminoalkyl radicals ( $\text{TEOH}_{(-\text{H})}$ ) as in reaction (4a). These observations are not consistent with the relevant photoinitiation ability of 15-DHAQ and 18-DHAQ based photoinitiating systems. This can be ascribed to the fact that a back electron

transfer reaction (reaction (4b)) occurred in the 15-DHAQ/TEOH based system, which diminished the relevant photoinitiation ability. For the 15-DHAQ (or 18-DHAQ)/Iod couple, however, no fluorescence quenching can be observed.

In laser flash photolysis experiments, no transient absorption of the triplet states of DHAQ was observed (Fig. S7 in the ESI†) indicating the very low intersystem crossing quantum yields. Therefore, the singlet route probably predominates in the DHAQ/additive interaction.

From steady state photolysis experiments under blue LED irradiation, no bleaching was observed for the 15-DHAQ/Iod or 18-DHAQ/Iod system in acetonitrile as shown in Fig. S5(a) and (b) in the ESI.† This may be ascribed to the back electron transfer reaction as indicated in reaction (2b). Interestingly, with the addition of NVK into the 18-DHAQ/Iod system in acetonitrile, the solution became turbid after only 10 s of blue LED irradiation [Fig. S5(c) in the ESI:† the baseline of the UV-vis absorption spectrum increased significantly after the light irradiation] indicating the production of an insoluble polymer (*i.e.* polyvinylcarbazole). It means that NVK can react with phenyl radicals as in reactions (5) and (6) and promoted the reactions (2a) and (3). This is also in agreement with the fact that DHAQ/Iod/NVK three-component systems were more efficient than DHAQ/Iod two-component systems (*e.g.* 14-DHAQ based systems, Fig. 3 and Table 2). On the other hand, the ground state absorption of the 18-DHAQ/TEOH system in acetonitrile decreased much more rapidly than that of the 15-DHAQ/TEOH system (Fig. 5) which is consistent with the higher photoinitiation ability of the 18-DHAQ based system.

Following the electron transfer in the DHAQ/Iod systems under light irradiation, the generated radicals can be observed directly by ESR spin trapping experiments. The hyperfine splitting (HFS) constants for both the nitrogen ( $a_{\text{N}}$ ) and the hydrogen ( $a_{\text{H}}$ ) of the PBN/radical adducts can be used to determine the specific radicals. For instance, in the 18-DHAQ/Iod system  $a_{\text{N}} = 14.2 \text{ G}$  and  $a_{\text{H}} = 2.1 \text{ G}$  were measured (Fig. 6), leading to the assignment of PBN/phenyl radical adducts,<sup>32,33</sup> which confirmed the production of phenyl radicals ( $\text{Ph}^{\bullet}$ ) as in reactions (1)–(3).



Fig. 5 Steady state photolysis of (a) 15-DHAQ/TEOH and (b) 18-DHAQ/TEOH in acetonitrile ( $[\text{TEOH}] = 60 \text{ mM}$ ) under irradiation of blue LED@455 nm; UV-vis spectra recorded at different irradiation times.



Fig. 6 ESR spectra of the radicals generated in 18-DHAQ/Iod upon exposure to the LED@455 nm and trapped by PBN in tert-butylbenzene: (a) experimental and (b) simulated spectra.

### Free radical photopolymerization of monofunctional monomers on DHAQ-based photoinitiating systems

Very recently, conventional UV light sensitive radical photoinitiators have been reported to induce photoRAFT polymerizations and it indicates that the types of photoinitiators and experimental conditions are of importance to achieve good results.<sup>34</sup> In this study, the phenyl radicals generated from the 18-DHAQ/Iod system during blue LED irradiation can initiate the free radical photopolymerization of DEGMEMA as expected. Specifically, after 2 h of blue LED irradiation, poly(DEGMEMA) (Fig. 7a) with a molecular weight of  $M_n = 31\,100 \text{ g mol}^{-1}$  in the 18-DHAQ/Iod/DEGMEMA system ([18-DHAQ]:[Iod]:[DEGMEMA] = 0.2 : 0.8 : 100) can be obtained. As expected for a free radical polymerization the dispersity was high ( $D = 1.75$ ). The addition of a RAFT agent (CPADB) to the photopolymerization of DEGMEMA ([18-DHAQ]:[Iod]:[CPADB]:[DEGMEMA] = 0.2 : 0.8 : 1 : 100) led to the formation of well-controlled poly(DEGMEMA) ( $M_n = 7500 \text{ g mol}^{-1}$ ,  $D = 1.14$ ) after 4 h of blue LED irradiation (Fig. 7b) indicating that the phenyl radicals generated from 18-DHAQ/Iod



Fig. 7 SEC chromatograms of poly(DEGMEMA) synthesized in the presence of different photoinitiating systems (PISs) upon exposure to the blue LED.

can initiate the RAFT photopolymerization in the presence of CPADB. Moreover, RAFT photopolymerization of DEGMEMA can also be carried out using the 18-DHAQ/CPADB/DEGMEMA system ([18-DHAQ]:[CPADB]:[DEGMEMA] = 0.2 : 1 : 100) under blue LED irradiation. Precisely, poly(DEGMEMA) ( $M_n = 5600 \text{ g mol}^{-1}$ ) with low dispersity ( $D = 1.15$ ) was obtained after 4 h of blue LED exposure (Fig. 7c). It demonstrated that Iod was not necessary in the system for the RAFT photopolymerization but accelerated the polymerization rate (*i.e.* a monomer conversion of 39.8% was obtained with 18-DHAQ/Iod/CPADB vs. 29.7% using 18-DHAQ/CPADB after 4 h irradiation).

### Cationic photopolymerization on DHAQ-based photoinitiating systems

As illustrated in reactions (1)–(3) and (5)–(6), DHAQ-derived cations (DHAQs<sup>+</sup>) and NVK-derived cations (NVKs<sup>+</sup>) are expected to be produced from DHAQ/Iod and DHAQ/Iod/NVK photoinitiating systems, respectively, when irradiated with blue LED. The photoinitiating ability of the systems for the cationic photopolymerization can be associated with the chemical structures of DHAQs and their reactivity with additive Iod as discussed above.

Similar to free radical photopolymerization described above, Iod or NVK alone yielded no cationic photopolymerization for EPOX under blue LED irradiation indicating the importance of the presence of DHAQs in the photoinitiating systems. As demonstrated in Table 2, 12-DHAQ based systems were inefficient for the cationic photopolymerization, which was also the case of free radical photopolymerization. It can be ascribed to the low solubility of 12-DHAQ in bulk EPOX. The two-component photoinitiating system 14-DHAQ/Iod yielded no polymerization of EPOX due to the back electron transfer reaction as discussed above. As expected, the three-component photoinitiating systems exhibited higher photoinitiating ability for cationic photopolymerization than that of the two-component systems; thanks to the excellent NVK additive effect.<sup>35</sup> The photoinitiating



Fig. 8 Photopolymerization profiles of EPOX under air in the presence of DHAQ/Iod/NVK (0.5%/2%/3%, wt%) upon exposure to the blue LED@455 nm.

ability of the three-component photoinitiating systems decreased as 18-DHAQ/Iod/NVK > 14-DHAQ/Iod/NVK > 15-DHAQ/Iod/NVK (Fig. 8), which is also consistent with the free radical photopolymerization. Markedly, the 18-DHAQ/Iod/NVK combination demonstrated the highest efficiency to initiate the cationic photopolymerization of EPOX (79% of conversion can be achieved after 800 s of light irradiation, and 62% can be attained after 120 s indicating the high polymerization rate) upon blue LED exposure. Furthermore, the occurrence of the cationic photopolymerization of EPOX can be confirmed by the consumption of the epoxy group ( $\sim 790\text{ cm}^{-1}$ ) and the concomitant formation of polyether ( $\sim 1070\text{ cm}^{-1}$ ) and hydroxyl ( $\sim 3430\text{ cm}^{-1}$ ) groups from the IR spectra (Fig. S8 in the ESI†).

## Conclusion

This research demonstrated that the positions of hydroxyl substituents in the anthraquinone molecule played an important role in their photoinitiation efficiency (evaluated by the functional group conversions of *ca.* 0.5–3  $\mu\text{m}$  depth of samples in contact with the ATR crystal) when combined with different additives. Among all the studied dihydroxyanthraquinone derivative-based photoinitiating systems, 18-DHAQ-based systems (*i.e.* 18-DHAQ/Iod/NVK and 18-DHAQ/TEAOH/R-Br) exhibited the highest photoinitiating ability for both free radical and cationic photopolymerizations under the irradiation of a blue LED bulb (conversion of 55% and 79% for free radical photopolymerization and cationic photopolymerization, respectively) while 12-DHAQ-based systems were inefficient due to their low solubility in monomers. Interestingly, a 14-DHAQ/Iod/NVK or an 18-DHAQ/Iod/NVK system could initiate the free radical photopolymerization upon exposure to the household green LED bulb, and the 14-DHAQ based combination was more efficient than the 18-DHAQ based system due to the more overlap between the light absorption of 14-DHAQ and the emission spectrum of the green LED bulb. The photochemical mechanism investigations revealed that the positions of hydroxyl substituents in the anthraquinone molecule significantly influenced their interaction reactivity with TEOH in the steady state photolysis processes, which was in agreement with their photoinitiating ability of the relevant systems. The fluorescence quenching of DHAQs by TEOH can also be observed due to the electron transfer reaction while no quenching of DHAQs by Iod indicated the occurrence of a back electron transfer reaction in the related systems. The addition of a second additive (*e.g.* NVK) can promote the electron transfer and thus improve the photoinitiation efficiency of the systems. Moreover, 18-DHAQ/Iod based photoinitiating systems can also initiate the free radical photopolymerization of a monofunctional monomer (DEGMEMA) while the controlled RAFT photopolymerization of DEGMEMA in bulk can also be conducted in the presence of a RAFT agent (CPADB) upon blue LED exposure. The investigation of various monomers in bulk and relevant photochemical mechanisms of the RAFT photopolymerization is in progress.

## Conflict of interest

The authors declare no competing financial interest.

## Acknowledgements

P. X. acknowledges funding from France–Australia Science Innovation Collaboration Fellowships (Rod Rickards Fellowship Scheme) of the Australian Academy of Science and the Faculty Research Grants at University of New South Wales. The authors acknowledge funding from the Australian Research Council (ARC).

## References

- 1 J. P. Fouassier and J. Lalevée, *Photoinitiators for Polymer Synthesis-Scope, Reactivity, and Efficiency*, Wiley-VCH Verlag GmbH & Co KGaA, Weinheim, 2012.
- 2 J. Lalevée and J. P. Fouassier, *Dyes and Chromophores in Polymer Science*, ISTE Wiley, London, 2015.
- 3 P. Xiao, J. Zhang, F. Dumur, M. A. Tehfe, F. Morlet-Savary, B. Graff, D. Gigmes, J. P. Fouassier and J. Lalevée, *Prog. Polym. Sci.*, 2015, **41**, 32–66.
- 4 N. S. Allen, *Photochemistry and photophysics of polymer materials*, John Wiley & Sons Inc., New York, 2010.
- 5 J. V. Crivello and K. Dietliker, *Photoinitiators for Free Radical, Cationic and Anionic Photopolymerization*, John Wiley & Sons, Chichester, 2nd edn, 1998.
- 6 C. Hiemstra, W. Zhou, Z. Zhong, M. Wouters and J. Feijen, *J. Am. Chem. Soc.*, 2007, **129**, 9918–9926.
- 7 S. Shi, P. Xiao, K. Wang, Y. Gong and J. Nie, *Acta Biomater.*, 2010, **6**, 3067–3071.
- 8 B. Derby, *Science*, 2012, **338**, 921–926.
- 9 L. García-Fernández, C. Herbivo, V. S. M. Arranz, D. Warther, L. Donato, A. Specht and A. del Campo, *Adv. Mater.*, 2014, **26**, 5012–5017.
- 10 H. Peng, S. Bi, M. Ni, X. Xie, Y. Liao, X. Zhou, Z. Xue, J. Zhu, Y. Wei, C. N. Bowman and Y.-W. Mai, *J. Am. Chem. Soc.*, 2014, **136**, 8855–8858.
- 11 M. Kaupp, A. S. Quick, C. Rodriguez-Emmenegger, A. Welle, V. Trouillet, O. Pop-Georgievski, M. Wegener and C. Barner-Kowollik, *Adv. Funct. Mater.*, 2014, **24**, 5649–5661.
- 12 T. Tischer, C. Rodriguez-Emmenegger, V. Trouillet, A. Welle, V. Schueler, J. O. Mueller, A. S. Goldmann, E. Brynda and C. Barner-Kowollik, *Adv. Mater.*, 2014, **26**, 4087–4092.
- 13 P. Xiao, C. Simonnet-Jégat, F. Dumur, G. Schrodj, M.-A. Tehfe, J. P. Fouassier, D. Gigmes and J. Lalevée, *Polym. Chem.*, 2013, **4**, 4526–4530.
- 14 P. Xiao, F. Dumur, M.-A. Tehfe, B. Graff, J. P. Fouassier, D. Gigmes and J. Lalevée, *Macromol. Chem. Phys.*, 2013, **214**, 1749–1755.

- 15 J. Zhao, J. Lalevee, H. Lu, R. MacQueen, S. H. Kable, T. W. Schmidt, M. H. Stenzel and P. Xiao, *Polym. Chem.*, 2015, **6**, 5053–5061.
- 16 R. Siva, *Curr. Sci.*, 2007, **92**, 916–925.
- 17 E. H. Anouar, C. P. Osman, J.-F. F. Weber and N. H. Ismail, *SpringerPlus*, 2014, **3**, 233.
- 18 P. Ghosh, G. P. Devi, R. Priya, A. Amrita, A. Sivaramakrishna, S. Babu and R. Siva, *Appl. Biochem. Biotechnol.*, 2013, **170**, 1127–1137.
- 19 C. Müller, J. Schroeder and J. Troe, *J. Phys. Chem. B*, 2006, **110**, 19820–19832.
- 20 P. Xiao, F. Dumur, B. Graff, J. P. Fouassier, D. Gigmes and J. Lalevée, *Macromolecules*, 2013, **46**, 6744–6750.
- 21 Y. Mitsukami, M. S. Donovan, A. B. Lowe and C. L. McCormick, *Macromolecules*, 2001, **34**, 2248–2256.
- 22 J. B. Foresman and A. Frisch, *Exploring Chemistry with Electronic Structure Methods*, Gaussian, Inc., 1996.
- 23 M. J. Frisch, G. W. Trucks, H. B. Schlegel, G. E. Scuseria, M. A. Robb, J. R. Cheeseman, V. G. Zakrzewski, J. A. Montgomery, J. R. E. Stratmann, J. C. Burant, S. Dapprich, J. M. Millam, A. D. Daniels, K. N. Kudin, M. C. Strain, O. Farkas, J. Tomasi, V. Barone, M. Cossi, R. Cammi, B. Mennucci, C. Pomelli, C. Adamo, S. Clifford, J. Ochterski, G. A. Petersson, P. Y. Ayala, Q. Cui, K. Morokuma, P. Salvador, J. J. Dannenberg, D. K. Malick, A. D. Rabuck, K. Raghavachari, J. B. Foresman, J. Cioslowski, J. V. Ortiz, A. G. Baboul, B. B. Stefanov, G. Liu, A. Liashenko, P. Piskorz, I. Komaromi, R. Gomperts, R. L. Martin, D. J. Fox, T. Keith, M. A. Al-Laham, C. Y. Peng, A. Nanayakkara, M. Challacombe, P. M. W. Gill, B. Johnson, W. Chen, M. W. Wong, J. L. Andres, C. Gonzalez, M. Head-Gordon, E. S. Replogle and J. A. Pople, *Gaussian 03, Revision B-2*, Gaussian, Inc., Pittsburgh PA, 2003.
- 24 P. Xiao, W. Hong, Y. Li, F. Dumur, B. Graff, J. P. Fouassier, D. Gigmes and J. Lalevée, *Polym. Chem.*, 2014, **5**, 2293–2300.
- 25 J. P. Fouassier, *Photoinitiator, Photopolymerization and Photocuring: Fundamentals and Applications*, Hanser Publishers, New York/Munich/Vienna, 1995.
- 26 J. Lalevée, N. Blanchard, M. A. Tehfe, M. Peter, F. Morlet-Savary, D. Gigmes and J. P. Fouassier, *Polym. Chem.*, 2011, **2**, 1986–1991.
- 27 P. Xiao, J. Lalevée, X. Allonas, J. P. Fouassier, C. Ley, M. El Roz, S. Q. Shi and J. Nie, *J. Polym. Sci., Part A: Polym. Chem.*, 2010, **48**, 5758–5766.
- 28 P. Xiao, F. Dumur, M. Frigoli, M.-A. Tehfe, F. Morlet-Savary, B. Graff, J. P. Fouassier, D. Gigmes and J. Lalevée, *Polym. Chem.*, 2013, **4**, 5440–5448.
- 29 H. Pal, D. K. Palit, T. Mukherjee and J. P. Mittal, *J. Chem. Soc., Faraday Trans.*, 1993, **89**, 683–691.
- 30 M. P. Marzocchi, A. R. Mantini, M. Casu and G. Smulevich, *J. Chem. Phys.*, 1998, **108**, 534–549.
- 31 P. Dahiya, M. Kumbhakar, T. Mukherjee and H. Pal, *J. Mol. Struct.*, 2006, **798**, 40–48.
- 32 M. A. Tehfe, J. Lalevée, S. Telitel, E. Contal, F. Dumur, D. Gigmes, D. Bertin, M. Nechab, B. Graff, F. Morlet-Savary and J. P. Fouassier, *Macromolecules*, 2012, **45**, 4454–4460.
- 33 J. Lalevée, N. Blanchard, M. A. Tehfe, F. Morlet-Savary and J. P. Fouassier, *Macromolecules*, 2010, **43**, 10191–10195.
- 34 B. Wenn and T. Junkers, *Macromolecules*, 2016, **49**, 6888–6895.
- 35 J. Lalevée, M.-A. Tehfe, A. Zein-Fakih, B. Ball, S. Telitel, F. Morlet-Savary, B. Graff and J. P. Fouassier, *ACS Macro Lett.*, 2012, **1**, 802–806.